Angewandte Chemie
Eine Zeitschrift der Gesellschaft Deutscher Chemiker

Supporting Information

Because the Light is Better Here: Correlation-Time Analysis by NMR Spectroscopy

Albert A. Smith, Matthias Ernst, and Beat H. Meier**

ange_201707316_sm_miscellaneous_information.pdf

Table of Contents

Calculation of rate constants 2

Table of calculation parameters 3

Two Dimensional plots of fit error 3

Fit error nearby and far from sensitive correlation times 7

Biasing in R_1 measurements 7

Calculating $R_{1\rho}$ correlation time bias 8

Correlation time biasing in multi-timescale fits 10

Detectors 13

References 14

Calculation of rate constants

Rate constants are calculated from the correlation function, which is assumed to be a sum of exponentials,[1] generally written as:

$$C(t)=\frac{2}{5}\left[S^2+(1-S^2)\sum_{i=1}A_i\exp(-t/\tau_i)\right] \tag{1}$$

S^2 is the order parameter, where $1–S^2$ is related to the total amplitude of the internal motion, and the A_i give the contributions of each individual exponential to the total motion, such that $\sum A_i=1$. Then, to calculate rate constants, one needs the spectral density function, $J(\omega)$, which is the Fourier transform of the correlation function:

$$J(\omega)=\frac{2}{5}(1-S^2)\sum_{i=1}A_i\frac{\tau_i}{1+(\omega\tau_i)^2}\ . \tag{2}$$

R_1 and $R_{1\rho}$ rate constants, used as examples in the main text, can be calculated as follows:[2]

$$R_1=\left(\frac{\delta_{IS}}{4}\right)^2\left(J(\omega_I-\omega_S)+3J(\omega_I)+6J(\omega_I+\omega_S)\right)+\frac{3}{4}\left(\omega_I\sigma_{zz}\right)^2J(\omega_I) \tag{3}$$

Here, R_1 gives the longitudinal relaxation-rate constant of spin I, which is dipole-coupled to spin S, with coupling constant δ_{IS}. Then, ω_I and ω_S are the Larmor frequencies of the I and S spins respectively. Finally, $\omega_I\sigma_{zz}$ is the zz-component of the chemical shift anisotropy (CSA) tensor (σ_{zz}=2/3$\Delta\omega$, the full width of the CSA tensor). All terms are given in radians/second and the resulting rate constant is in s^{-1}. $R_{1\rho}$ is calculated as follows:[3]

$$\begin{aligned}R_{1\rho}=&\frac{1}{2}R_1+\\&\left(\frac{\delta^{IS}}{4}\right)\left(3J(\omega_S)+\frac{1}{3}J(\omega_1-2\omega_r)+\frac{2}{3}J(\omega_1-\omega_r)+\frac{2}{3}J(\omega_1+\omega_r)+\frac{1}{3}J(\omega_1+2\omega_r)\right)\\&+\frac{1}{6}\left(\omega_I\sigma_{zz}\right)^2\left(\frac{1}{2}J(\omega_1-2\omega_r)+J(\omega_1-\omega_r)+J(\omega_1+\omega_r)+\frac{1}{2}J(\omega_1+2\omega_r)\right)\end{aligned} \tag{4}$$

Here, ω_1 is the field strength of a spin-locking field, which is applied on resonance to spin I. ω_r is the magic angle spinning frequency. Both are given in radians/second.

Table of calculation parameters

Location	R_1 Parameters	$R_{1\rho}$ Parameters	S^2
Figure 1A	$\omega_{0H}/2\pi$=400, 500, 850 MHz	—	—
Figure 1B	$\omega_{0H}/2\pi$=400, 500, 850 MHz	—	✓
Figure 1C	$\omega_{0H}/2\pi$=400, 500, 850 MHz	$\omega_{0H}/2\pi$=850 MHz, $\omega_r/2\pi$=60 kHz,ω_1=15 kHz	—
Figure 1D	$\omega_{0H}/2\pi$=400, 500, 850 MHz	$\omega_{0H}/2\pi$=850 MHz, $\omega_r/2\pi$=60 kHz,ω_1=15 kHz	✓
Figure 1E	$\omega_{0H}/2\pi$=400, 500, 850 MHz	$\omega_{0H}/2\pi$=850 MHz, $\omega_r/2\pi$=60 kHz,ω_1=15, 25, 48 kHz	—
Figure 1F	$\omega_{0H}/2\pi$=400, 500, 850 MHz	$\omega_{0H}/2\pi$=850 MHz, $\omega_r/2\pi$=60 kHz,ω_1=15, 25, 48 kHz	□
Figure 2	—	$\omega_{0H}/2\pi$=850 MHz, ω_r=0.5*ω_r^0, ω_r^0,1.5* ω_r^0, ω_1=5 kHz	—
Figure 3	$\omega_{0H}/2\pi$=400, 500, 850 MHz	—	—
Figure 4	$\omega_{0H}/2\pi$=400, 600, 850 MHz	$\omega_{0H}/2\pi$=850 MHz, $\omega_r/2\pi$=60 kHz, ω_1=11, 16, 25, 38, 51 kHz	✓
SI Figure 3	$\omega_{0N}/2\pi=2/3\omega_N^0$, ω_N^0, $4/3\omega_N^0$	—	—
SI Figure 6	$\omega_{0H}/2\pi$=500, 750, 1000 MHz	$\omega_{0H}/2\pi$=750 MHz, $\omega_r/2\pi$=45, 90, 135 kHz, $\omega_1/2\pi$=5 kHz	—
SI Figure 8	$\omega_{0H}/2\pi$=400, 600, 850 MHz	$\omega_{0H}/2\pi$=850 MHz, $\omega_r/2\pi$=60, $\omega_1/2\pi$=10 kHz	✓

All calculations assume δ_{IS}=-22.945 kHz, and $\omega_I\sigma_{zz}$=113 ppm.

Two Dimensional plots of fit error

Main text Figure 1 shows the optimum fitting for a number of types of data sets and motional models. However, the resulting plots represent only the best fit, but do not indicate how well defined the minimum is. Therefore, we plot the error of the fit, χ^2, as a function of τ_c and $(1–S^2)A_i$ for each exponential in the correlation function. Our χ^2 is calculated according to

$$\chi^2 = \sum_{i=1}^{N} \frac{(O_i - C_i)^2}{\sigma_i^2} \tag{5}$$

where O_i and C_i are the observed and calculated values (here the initial calculation and the calculation for fitting, respectively). σ_i^2 is the standard deviation of the measurement, which we have assumed to be 10% of the median initial value for that data type (R_1, $R_{1\rho}$, S^2). Note that for multiexponential fit models, parameters not shown as axes are optimized.

Table of initial model parameters for main text Figure 1, SI Figure 1

	A/B	C/D	E/F
Input: τ_c	10^{-8} s,10^{-10} s	10^{-6} s, 10^{-8} s, 10^{-10}	$10^{-5.5}$ s, 10^{-8} s, 10^{-10} s, 10^{-12} s
Input: $(1–S^2)A_i$	0.0900, 0.1000	0.0086, 0.0450, 0.1000	0.0079, 0.0415, 0.0675, 0.1000
Number of exponentials in model	2	3	4
Number of exponentials in fit	1	2	3

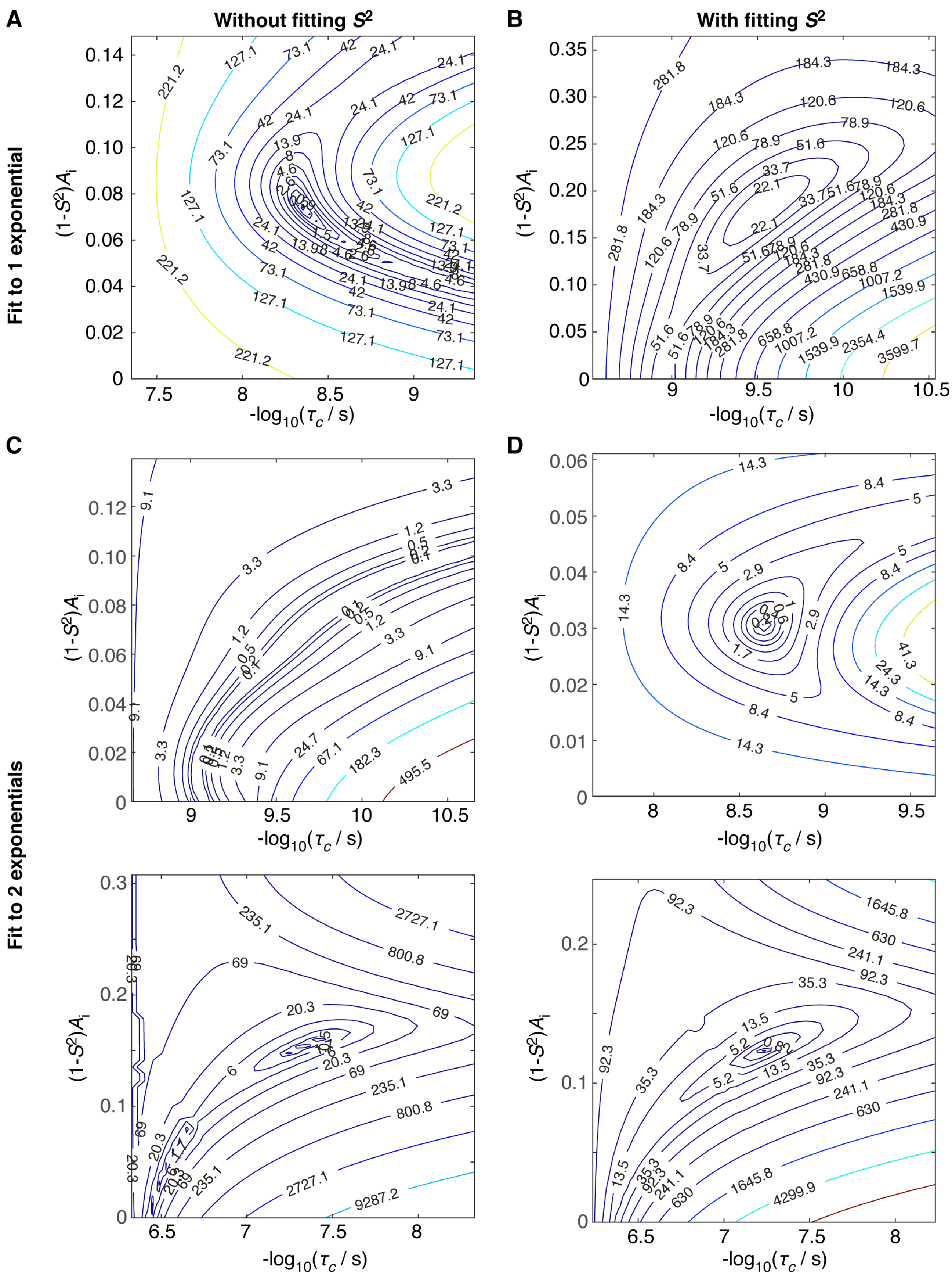
A
Without fitting S^2
B
With fitting S^2
C
D
Fit to 1 exponential
Fit to 2 exponentials
$(1-S^2)A_i$
$-\log_{10}(\tau_c\ /\ s)$

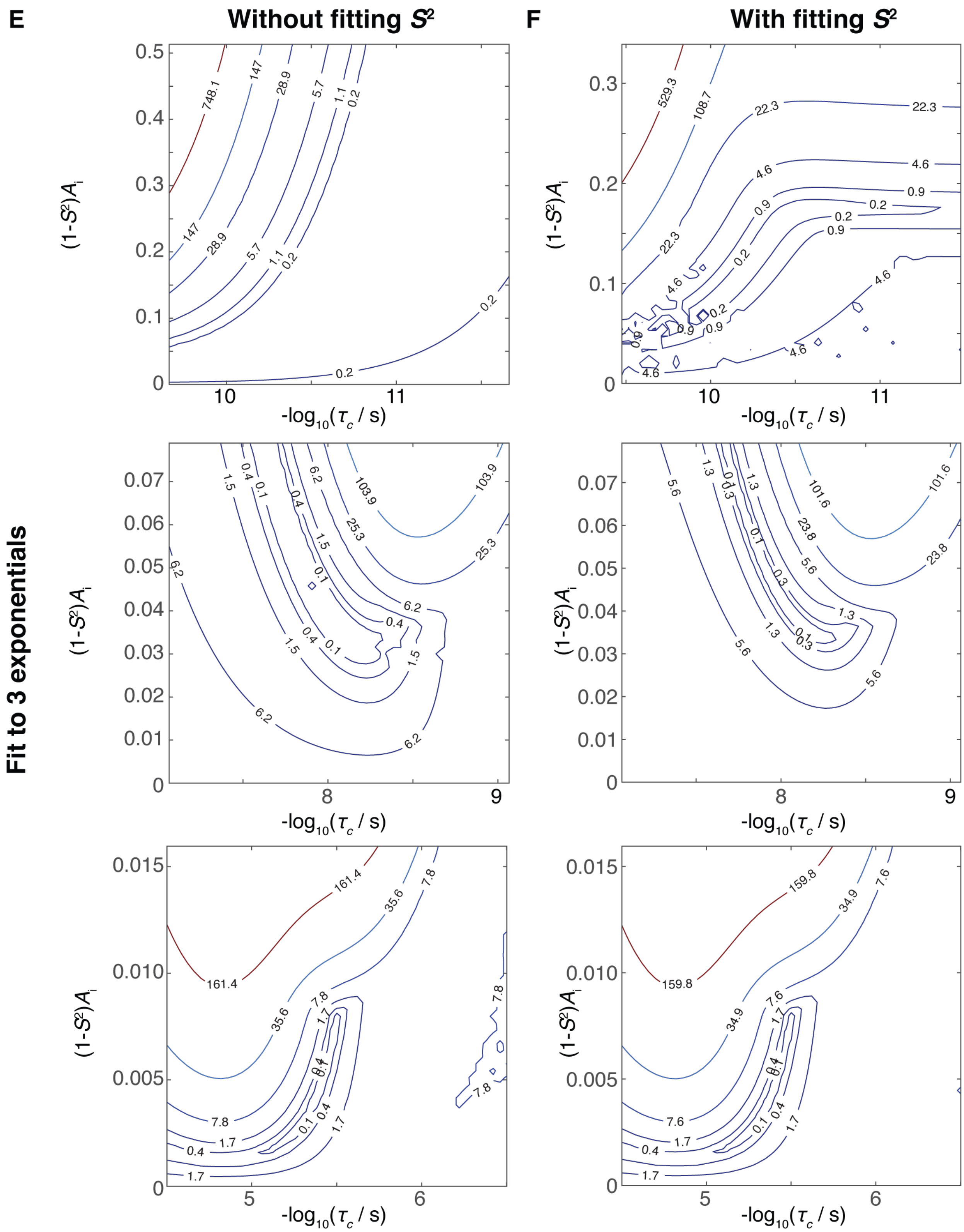

SI Figure 1. 2D χ^2 plots corresponding to main text Figure 1. In each plot, the amplitude, (1-S^2)A_i, and correlation time (τ_c) of one exponential term in the correlation function is varied, with contours giving the χ^2 value. Other parameters in the correlation function are re-optimized at each amplitude/correlation time pair. **A**/**B** shows the χ^2 surface for fitting with one exponential term, **B**/**C** for two terms, and **E**/**F** for three terms. **A**, **C**, and **E** are fitted without the total S^2, **B**, **D**, and **F** are fitted with the total S^2 (corresponding to the sections in text Figure 1).

One sees in SI Figure 1A/B that in both cases, a well-defined minimum is found for fits of three R_1 to a mono-exponential correlation function. However, when S^2 is fitted (B), then the minimum is not a good fit, as was also seen in main text Figure 1. In SI Figure 1C/D, where a bi-exponential correlation function is fit to three R_1 and one $R_{1\rho}$, a well-defined minimum only emerges when S^2 is included in the fit. In SI Figure 1E/F, where a tri-exponential correlation function is fitted to 3 R_1 and 3 $R_{1\rho}$, the minimum is rather broad even when including S^2. However, this is not so surprising- our recent work fitting relaxation data to a tri-exponential correlation function required setting the slowest correlation time to the same value for all residues in the HET-s(218-289) fibril, in order to obtain a well-defined minimum.[4]

We note that for all sections of text Figure 1, except B, if we were to add an additional exponential to the fitted correlation function (so that the initial correlation function had the same number of terms as the fitted correlation function), then we would have more fit parameters than experiments to fit to. In this case, multiple solutions would yield perfect fits so that we would not be able to reliably reproduce the original correlation function. In SI Figure 2, we plot the χ^2 surface resulting from fitting the data from text Figure 1B to a bi-exponential correlation function. We see for the two exponentials that the resulting χ^2 surfaces still exhibit very broad minima, so that increasing the number of exponential terms in the model is still not a viable option.

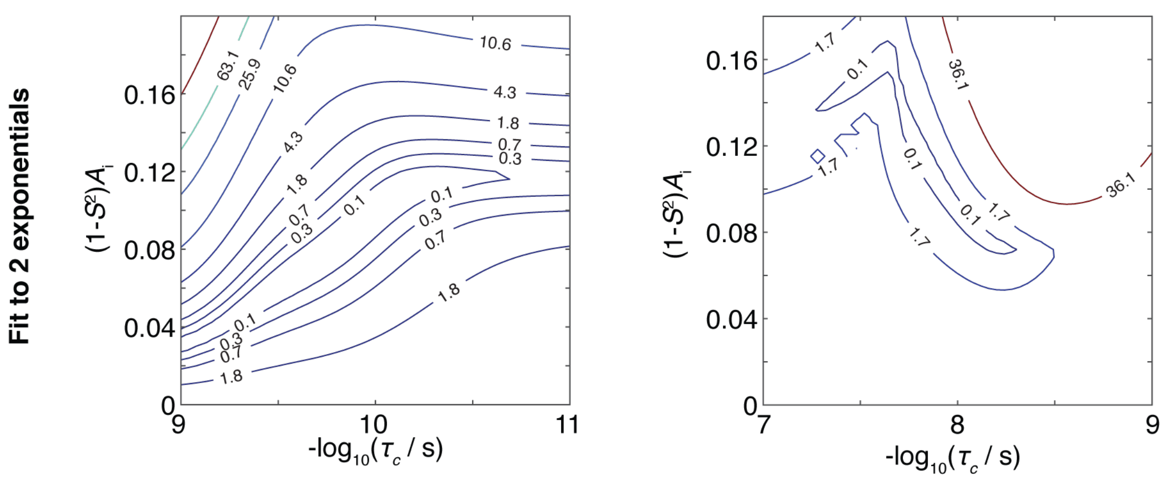

SI Figure 2. 2D χ^2 plots, where an initial bi-exponential correlation function is fitted to a model that is also bi-exponential, using 3 R_1 rate constants (400, 500, 850 MHz), and 1 S^2 value. The amplitude, $(1\text{-}S^2)A_i$, and correlation time (τ_c) of each exponential term in the correlation function is varied, with contours giving the χ^2 value. Parameters for the other exponential are re-optimized at each amplitude/correlation time pair. The initial correlation function is the same as found in text Figure 1B.

Fit error nearby and far from sensitive correlation times

We have shown that $R_{1\rho}$ or R_1 data resulting from a uniform distribution of motion, when fitted to the model given in SI eq. (6), is biased towards where the experiments are most sensitive. We also note that if we take our initial distribution of motion to have exactly one correlation time, and our fit to similarly have one correlation time, we find the slope of the error (χ^2, see SI eq. (5)) is much higher when the initial motion is near where the experiment is most sensitive. This can be seen in SI Figure 3, where we have fitted ^{15}N R_1 (400, 500, 850 MHz) resulting from a mono-exponential correlation function. In A, we assume $\tau_c=10^{-8.5}$ s, and then plot χ^2 as a function of $(1-S^2)A_i$ and τ_c, where we see that the fit has a very well-defined minimum. However, in B, we assume $\tau_c=10^{-7.5}$ s, and see that the minimum is not well-defined. This is because the ratio of R_1 rate constants is nearly constant for τ_c longer than ~10^{-8} s. Then, one obtains a good fit of R_1 for any correlation time in this range by increasing or decreasing the total amplitude of motion- resulting in highly correlated fit values between $(1-S^2)A_i$ and τ_c.

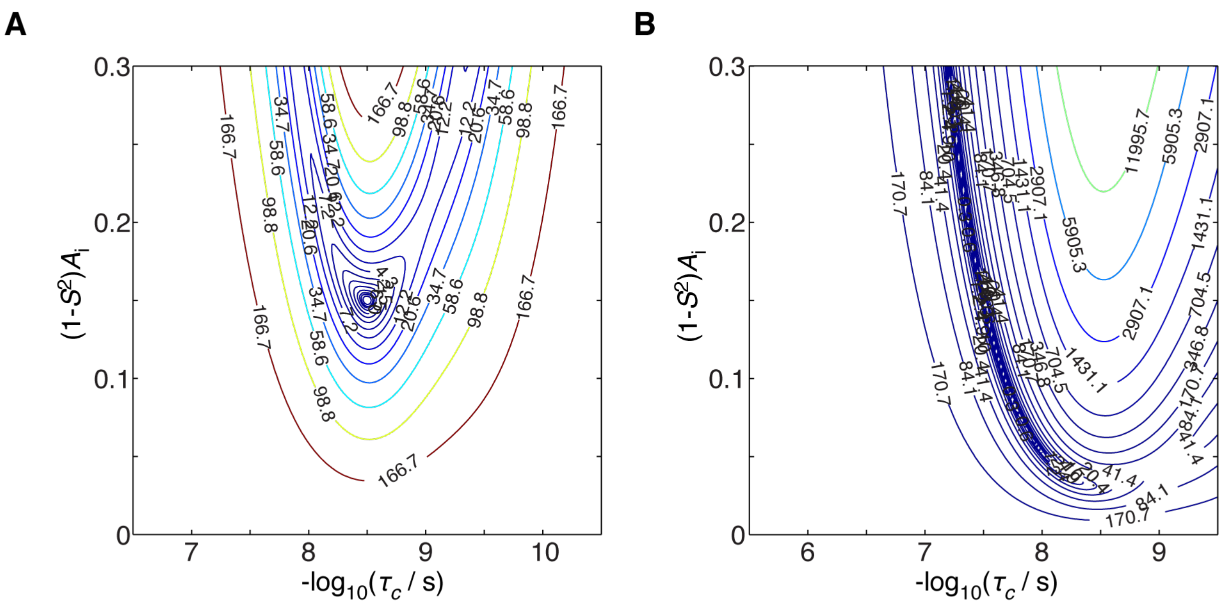

SI Figure 3: χ^2 for the fitting of three R_1 rate constants (400, 500, 850 MHz) to a mono-exponential correlation function, as a function of $(1-S^2)A_i$ and τ_c. In **A**, the input exponential has amplitude $(1-S^2)A_i=0.15$ and $\tau_c=10^{-8.5}$ s, where the R_1 experiments are most sensitive (see main text Figure 3A). **B** uses an exponential with the same amplitude, but $\tau_c=10^{-7.5}$ s.

Biasing in R_1 measurements

The tendency to bias towards where a set of experiments is most sensitive was demonstrated in Figure 2, where three $R_{1\rho}$ rate constants were calculated from a uniform distribution of motion, and then fitted to a mono-exponential correlation function, for varying experimental conditions. Using the same procedure, we calculate ^{15}N R_1 rate constants for a uniform distribution of motion, as a function of magnetic field, where the three fields are swept together (as a function of ω_N^0, where ω_N is the ^{15}N Larmor frequency). One similarly finds that the fitted correlation time is given approximately by $\tau_c \approx 1/\omega_N^0$, as shown in SI Figure 4.

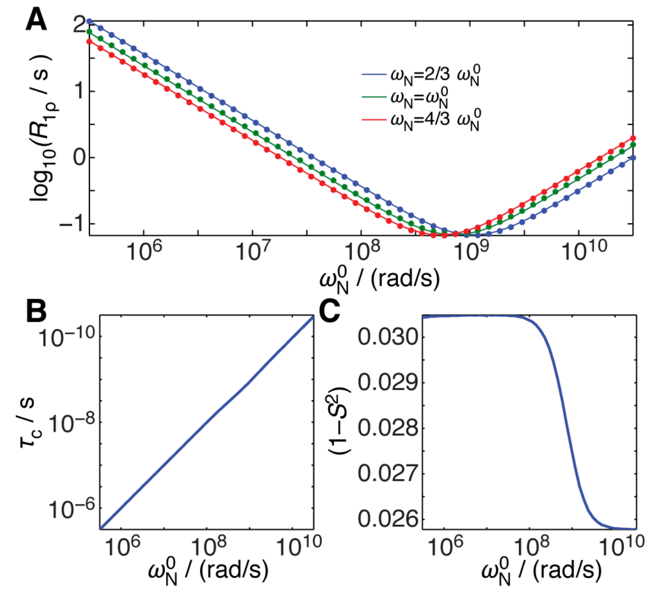

SI Figure 4. Fitting behavior as a function of experimental settings. A uniform distribution of motion is used to calculate 3 ^{15}N R_1 rate constants at different external fields (ω_N=2/3ω_N^0, ω_N^0, and 4/3ω_N^0). $\omega_N^0/2\pi$ is swept from 50 kHz to 5 GHz, where the calculated rate constants are shown in **A** (lines). The rate constants are well-fitted with a mono-exponential correlation function (**A**, circles), with the fitted correlation time (τ_c) shown in **B**, and amplitude, (1–S^2), shown in **C**.

Calculating $R_{1\rho}$ correlation time bias

To calculate what correlation time a set of experiments is biased towards, we first assume a uniform distribution of motion, specifically, by taking 200 values of τ_i logarithmically spaced between 10^{-14} s and 10^{-3} s, and setting the corresponding A_i to all be equal (A_i=1/200, S^2=0 although S^2 does not affect τ_c result). We then calculate $R_{1\rho}$ for the set of experiments, according to Eqs. (2) and (4). This is then fitted. In the case of Figure 2, we used the following correlation function for fitting:

$$C(t) = \frac{2}{5}\left[S^2 + (1-S^2)\exp(-t/\tau_c)\right] \tag{6}$$

This correlation function was also used for fitting $R_{1\rho}$ calculated for MPD crystallized Ubiquitin, as was done in the original study by Lakomek et al.[5] The fitting procedure introduced by Smith et al. was used for fitting HET-s(218-289) ^{15}N and ^{13}Cα $R_{1\rho}$ data,[4] and for fitting PEG crystallized Ubiquitin.[6] In this case, the total $R_{1\rho}$ is assumed to be given by

$$R_{1\rho} = R_{1\rho}^{0} + R_{1\rho}(\omega_r, \omega_1, S^2, \tau_c) \tag{7}$$

where $R_{1\rho}^{0}$ is the relaxation contribution for nanosecond motions and is assumed to be equal for all experimental conditions, and $R_{1\rho}(\omega_r, \omega_1, S^2, \tau_c)$ is the relaxation contribution from slower motions, and changes depending on experimental conditions according to Eqs. (2) and (4). Fits for each of the experimental data sets are then shown in SI Figure 5.

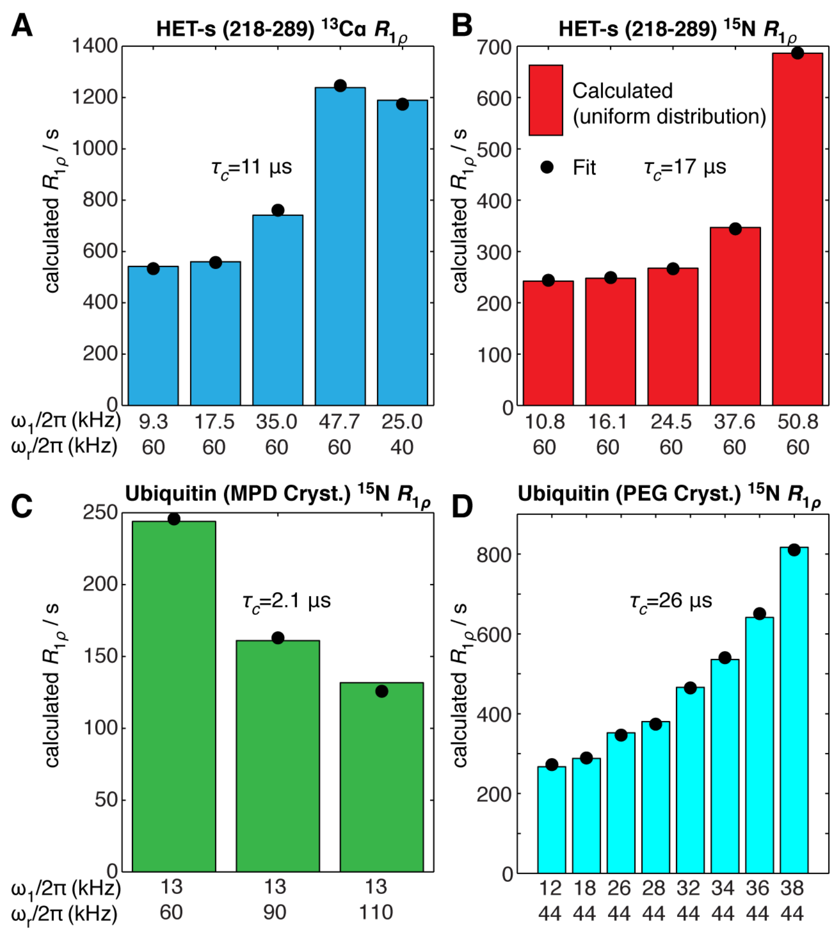

SI Figure 5. Determination of biasing tendencies for different data sets. In **A-D**, a uniform distribution of motion is assumed, and $R_{1\rho}$ is calculated for different conditions (bars), where the spin-lock strengths and spinning frequencies are specified below the bar plots. These are fitted to a model of motion (fit shown as filled circles), to obtain the correlation time towards which motional models will be biased (τ_c given in plots). **A** HET-s(218-289) ^{13}Cα $R_{1\rho}$,[4] **B** HET-s(218-289) ^{15}N $R_{1\rho}$,[4] **C** Ubiquitin (MPD crystalized),[5] **D** Ubiquitin (PEG crystalized).[6]

Correlation time biasing in multi-timescale fits

In the case that several R_1 and several $R_{1\rho}$ rate constants are measured, and fitted to a bi-exponential correlation function, one finds that the two τ_c tend towards the two centers where R_1 and $R_{1\rho}$ are most sensitive. We show this by calculating ^{15}N R_1 at several fields (500, 750, 1000 MHz), and $R_{1\rho}$ at several spinning frequencies (45, 90, 135 kHz, with $\omega_1/2\pi$ = 5 kHz and $\omega_{0H}/2\pi$=750 MHz), assuming a uniform distribution (SI Figure 6A, bars). These can then be fitted to a bi-exponential correlation function, with the fit quality shown (Figure 3A, circles). The resulting correlation times fall at $10^{-8.6}$ and $10^{-5.7}$ s (SI Figure 6B, red line). These are nearly identical to those found when fitting only R_1 or only $R_{1\rho}$ to a mono-exponential correlation function (SI Figure 6B, circles). Additionally, they correspond approximately to where the R_1 and $R_{1\rho}$ experiments are most sensitive (SI Figure 6C).

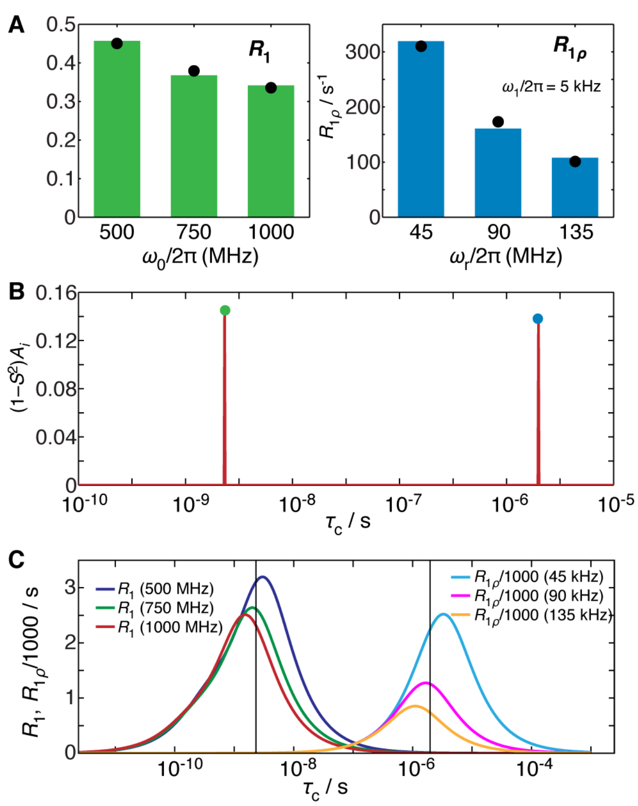

SI Figure 6. Fitting multiple R_1 and $R_{1\rho}$ rate constants to a bi-exponential correlation function. **A** shows the rate constants resulting from a uniform distribution of motion (τ_i distributed logarithmically from 10^{-14} and 10^{-3} s with equal A_i, S^2=0) (bars). Filled circles in **A** show the fit quality to a bi-exponential correlation function. **B** shows the correlation times and amplitudes of the fit, where circles show the correlation times and amplitudes found when fitting only R_1 or only $R_{1\rho}$ to a mono-exponential correlation function. **C** shows R_1 and $R_{1\rho}$ as a function of τ_c for a mono-exponential correlation function, with S^2=0, where vertical lines mark the correlation times found in **B**.

In the case that several R_1 rate constants, an order parameter, S^2, and transverse relaxation (for example, $R_{1\rho}$) are fitted to a bi-exponential correlation function, the behavior changes considerably. As was shown in the text (Figure 3), if one correlation time is fixed to $10^{-10.5}$ s and the other to $10^{-7.5}$ s, then it is possible to fit R_1 rate constants at typical fields (400-1000 GHz) by adjusting the amplitudes of the two terms in the correlation function (text eq. (5)). This is because these correlation times give nearly the maximum and minimum possible ratios of the R_1 rate constants. Then, any ratio in between can be obtained from a weighted sum of the two τ_c, although for three rate constants this cannot be done exactly with only two variables (as seen by slight mis-fitting in Figure 3A). The ratios of R_1 rate constants are shown in SI Figure 7 (for ^{15}N R_1 at 400, 500, and 850 MHz).

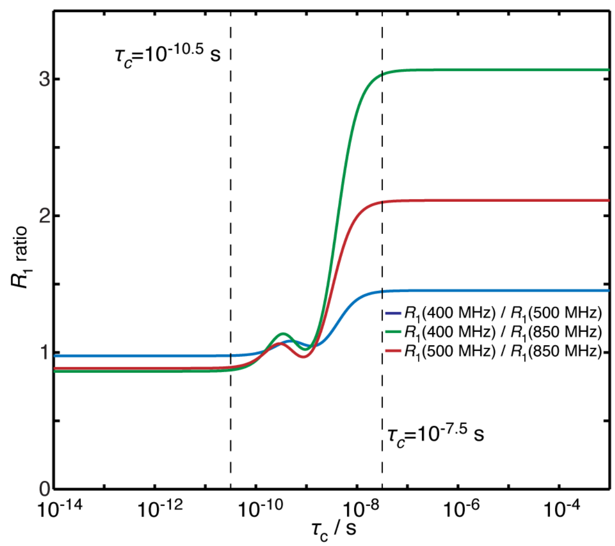

SI Figure 7. Ratio of R_1 rate constants as a function of correlation time. R_1 ratios are plotted for ^{15}N R_1 at 400, 500, and 850 MHz. Dashed lines mark $\tau_c=10^{-7.5}$ s and $10^{-10.5}$ s, although these ratios are nearly converged for $\tau_c<10^{-10}$ s and $\tau_c>10^{-8}$ s.

Fitting behavior when including S^2 and transverse relaxation differs because the two-timescale model must also fit these two experimental measurements. It is possible to fit any set of R_1 rate constants if one has one $\tau_c<10^{-10}$ s and the other $\tau_c>10^{-8}$ s (although not always perfect fit- see text Figure 3). To also fit S^2 and a transverse relaxation-rate constant, one could use the following procedure: 1) Fit R_1 rate constants using $\tau_c=10^{-10.5}$ s and $10^{-7.5}$ s, as in text eq. (5). 2) Calculate the transverse relaxation-rate constant. If the rate constant is too small, increase the longer τ_c (originally set to $10^{-7.5}$ s), while simultaneously increasing $(1–S^2)A_2$ (leave $(1–S^2)A_1$ fixed). This will increase the calculated transverse rate constant while leaving the R_1 fit unchanged (see SI Figure 6C, where increasing the τ_c from $10^{-7.5}$ s decreases all R_1 rate constants, but increases the $R_{1\rho}$ rate constants). 3) Similarly, if the calculated S^2 is larger than the experimental S^2, one may decrease the short τ_c while simultaneously increasing $(1–S^2)A_1$ (leave $(1–S^2)A_2$ fixed). This leaves the fit of R_1 rate constants unchanged, while decreasing S^2. Both steps 2) and 3) can also be inverted if the calculated transverse rate constant is too large or the S^2 is too small. Note that although algorithms used for fitting dynamics data do not explicitly take this approach, they appear to be arriving at the same fit. Also, if the real motion actually has a bi-exponential correlation function, then the correct fit should be nonetheless the best fit, although the fit using the method proposed here may have comparable fit quality, especially if signal-to-noise is low.

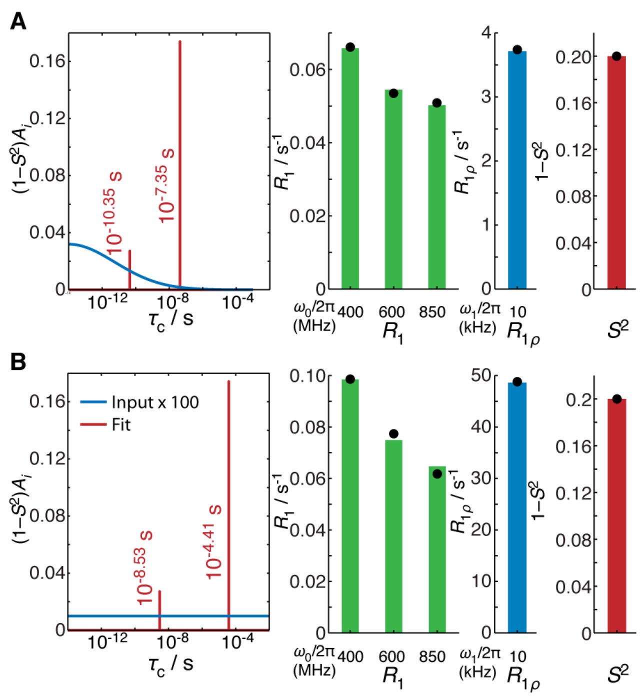

SI Figure 8. Fits of motional distributions to bi-exponential correlation function, with several R_1, one $R_{1\rho}$, and one S^2 fitted. In **A** and **B**, a distribution of motion is assumed (left, blue lines), and used to calculate R_1 at 400, 600, and 850 MHz, $R_{1\rho}$ at 850 MHz, with $\omega_r/2\pi$ =60 kHz and $\omega_1/2\pi$=10 kHz, and S^2 (right, bars). This is fitted assuming a bi-exponential correlation function (left, red lines), with the fit quality shown (right, circles). **A** shows fits of a log-Gaussian distribution of motion, and **B** shows fits of a uniform distribution of motion.

A fit is performed this way where we have assumed a log-Gaussian distribution of motion, calculated three R_1 rate constants, an $R_{1\rho}$ rate constant, and the order parameter S^2. The resulting fit has correlation times of $10^{-10.35}$ s and $10^{-7.35}$ s, as shown in SI Figure 8A, similar to the values of $10^{-10.5}$ s and $10^{-7.5}$ s often found in literature. Bear in mind that these are not the only possible values – their reoccurrence suggests a degree of universality to the real motion. However, in the case that the real motion involves more correlation times than the model, it is likely that they do not represent the real motion very well, as was seen in Figure 1.

Note that it is not possible to fit *any* distribution of motion this way, however, since we are limited in how far we may move the two correlation times. For example, a uniform distribution of motion can be fitted with two correlation times, as shown in SI Figure 8B. In this case, one correlation time fits the R_1 rate constants, falling approximately where the R_1 rate constants are most sensitive ($10^{-8.53}$ s), and the second correlation time falls far away from this region, at $10^{-4.41}$ s and simultaneously fits the $R_{1\rho}$ and order parameter. One would typically regard the lack of motion at shorter correlation times unphysical, but nonetheless highlights the unpredictable behavior of the bi-exponential correlation function for dynamics fitting.

Detectors

If we consider a correlation function given by a distribution function, such that

$$C(t) = (1-S^2)\int_0^\infty \theta(\tau_c)\exp(-t/\tau_c)d\tau_c\ , \qquad (8)$$

then any relaxation-rate constant may be calculated by taking the integral of the distribution function multiplied by $R_\zeta(\tau_c)$.

$$R_\zeta = (1-S^2)\int_0^\infty \theta(\tau_c)R_\zeta(\tau_c)d\tau_c\ , \qquad (9)$$

$R_\zeta(\tau_c)$ is the sensitivity of a rate constant, for some set of experimental conditions (specified by ζ), obtained by calculating the rate constant for a mono-exponential correlation function with correlation time τ_c and order parameter S^2=0 ($R_\zeta(\tau_c)$ is plotted in the text Figure 3A (lines) for several R_1 experiments). A rate constant on its own then characterizes motion where $R_\zeta(\tau_c)$ is relatively large. However, this may be a broad range of correlation times, and different rate constants may cover similar ranges of correlation times. Then we take advantage of the following property:

$$aR_\zeta + bR_\chi = (1-S^2)\int_0^\infty \theta(\tau_c)\left(aR_\zeta(\tau_c) + bR_\chi(\tau_c)\right)d\tau_c\ . \qquad (10)$$

We make the following definitions, which when inserted into eq. (10), yield text eq. (4).

$$\begin{aligned}\rho^{(\theta,S)} &= aR_\zeta + bR_\chi \\ \rho(\tau_c) &= aR_\zeta(\tau_c) + bR_\chi(\tau_c)\end{aligned} \tag{11}$$

We can optimize a and b to get narrow ranges for two different $\rho(\tau_c)$, as has been done in SI Figure 9, taking ^{15}N R_1 at 400 and 850 MHz (see text Figure 3A).

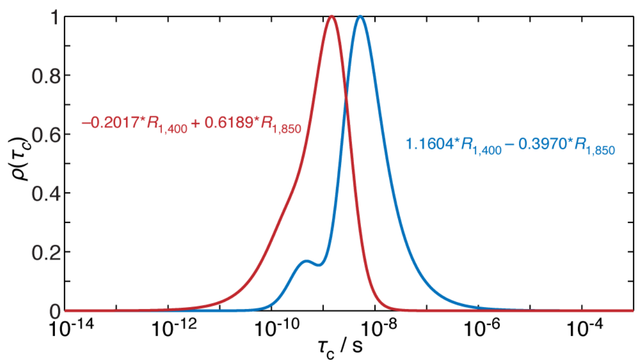

SI Figure 9. Linear combination of ^{15}N R_1 at 400 and 850 MHz to obtain two detectors, with sensitivities covering separated ranges of correlation times.

This approach is straightforward for a data set having only two rate constants, but in fact may be generalized for large data sets with mixed types of relaxation data. Methods of optimizing detectors for such data sets will be discussed in a separate report. Once detectors are optimized, then the detector response is given simply by eq. (11), which then may be used to characterize motion in the range where its sensitivity is large.

References

[1] G. Lipari, A. Szabo, *J. Am. Chem. Soc.* **1982**, *104*, 4559-4979.

[2] a) A. G. Redfield, *IBM J. Res. Dev.* **1957**, *1*, 19-31; b) A. G. Redfield, *Adv. Magn. Res.* **1965**, *1*, 1-32.

[3] a) U. Haeberlen, J. S. Waugh, *Phys. Rev.* **1969**, *185*, 420-429; b) R. Kurbanov, T. Zinkevich, A. Krushelnitsky, *J. Chem. Phys.* **2011**, *135*, 184104 (184101-184109).

[4] A. A. Smith, E. Testori, R. Cadalbert, B. H. Meier, M. Ernst, *J. Biomol. NMR* **2016**, *65*, 171-191.

[5] N. A. Lakomek, S. Penzel, A. Lends, R. Cadalbert, M. Ernst, B. H. Meier, *Chemistry* **2017**, *23*, 9425-9433.

[6] V. Kurauskas, S. A. Izmailov, O. N. Rogacheva, A. Hessel, I. Ayala, J. Woodhouse, A. Shilova, Y. Xue, T. Yuwen, N. Coquelle, J. P. Colletier, N. R. Skrynnikov, P. Schanda, *Nat Commun* **2017**, *8*, 145.